

TY Pup: a low-mass-ratio and deep contact binary as a progenitor candidate of luminous red novae

T. Sarotsakulchai^{1,4,5}, S.-B. Qian^{1,2,3,4}, B. Soonthornthum⁵, X. Zhou^{1,2,3}, J. Zhang^{1,2,3},
D. E. Reichart⁶, J. B. Haislip⁶, V. V. Kouprianov⁶ and S. Poshyachinda⁵

huangbinghe@ynao.ac.cn

ABSTRACT

TY Pup is a well-known bright eclipsing binary with an orbital period of 0.8192 days. New light curves in $B, V, (RI)_C$ bands were obtained with the 0.61-m reflector robotic telescope (PROMPT-8) at CTIO in Chile during 2015 and 2017. By analysing those photometric data with the W-D method, it is found that TY Pup is a low-mass-ratio ($q \sim 0.184$) and deep contact binary with a high fill-out factor (84.3%). An investigation of all available times of minimum light including three new ones obtained with the 60-cm and the 1.0-m telescopes at Yunnan Observatories in China indicates that the period change of TY Pup is complex. An upward parabolic variation in the $O - C$ diagram is detected to be superimposed on a cyclic oscillation. The upward parabolic change reveals a long-term continuous increase in the orbital period at a rate of $dP/dt = 5.57(\pm 0.08) \times 10^{-8} \text{ d yr}^{-1}$. The period increase can be explained by mass transfer from the less massive component ($M_2 \sim 0.3M_\odot$) to the more massive one ($M_1 \sim 1.65M_\odot$). The binary will be merging when it meets the criterion that the orbital angular momentum is less than 3 times the total spin angular momentum, i.e., $J_{orb} < 3J_{rot}$. This suggests that the system will finally merge into a rapid-rotating single star and may produce a luminous red nova. The cyclic oscillation in the $O - C$ diagram can be interpreted by the light-travel time effect (LITE) via the presence of a third body.

Subject headings: binaries: close – binaries: eclipsing – stars: evolution – stars: individual (TY Pup)

¹Yunnan Observatories, Chinese Academy of Sciences, 650216 Kunming, China

²Key Laboratory of the Structure and Evolution of Celestial Objects, Chinese Academy of Sciences, 650216 Kunming, China

³Center for Astronomical Mega-Science, Chinese Academy of Sciences, 20A Datun Rd., Chaoyang District, Beijing, 100012, China

⁴University of Chinese Academy of Sciences, 19 A Yuquan Rd., Shijingshan, 100049 Beijing, China

⁵National Astronomical Research Institute of Thailand, Ministry of Science and Technology, Bangkok, Thailand

⁶Department of Physics and Astronomy, University of North Carolina, CB #3255, Chapel Hill, NC 27599, USA

1. Introduction

W UMa-type stars are short-period ($P < 1$ day) binaries where both component stars are filling the critical Roche lobe and possess a common envelope (e.g., Qian et al. 2017). They evolved from detached binary stars via angular momentum loss and/or a case A mass transfer (e.g., Qian et al. 2018). Low-mass-ratio and deep contact binaries are on the late evolutionary state of contact binary systems. They have a high fill-out factor ($f > 50\%$) and a very low mass ratio ($q < 0.25$) (Qian et al. 2005). This type of binary may be the progenitors of single rapidly-rotating stars (e.g. Kandulapati et al., 2015; Sriram et al., 2016, 2017; Li et al. 2017; Liao et al. 2017; Samec et al. 2011, 2018) and will produce a new type of stellar outburst, i.e., luminous red novae (e.g., Tylenda et al. (2011); Stepien (2011); Zhu et al. 2016; Molnar et al. (2017)). Contact binary V1309 Sco is an example of progenitors for this eruption. These properties make them an important source to understand the merging of binaries and to investigate the structure and evolution of contact binaries at the late stage. On the other hand, W UMa-type binaries have the shortest orbital period and the lowest angular momentum among main-sequence binary stars. Searching for and studying the third components of such systems can also provide more information of their formation and evolution because they may have played an important role during the origin and evolution of contact binaries by removing angular momentum from the central binaries (Qian et al. 2013a).

TY Pup (HIP 36683, HD 60265) is one of the bright contact binaries in southern hemisphere, which was discovered by Hertzsprung (1928). Campbell (1928) made the first photometric measurements and derived its period as 0.58071564 days. The first spectroscopic observations were performed by Struve (1950) and found two periodicities with periods of 0.58 and 9.7 days, respectively. Later, new photometric observations were carried out by Huruata et. al. (1957), but the results were unable to confirm either Struve’s value of zero epoch or his secondary period of 9.7 days. The correct period of TY Pup was derived by Van Houten (1971) as 0.819235 days, which fitted well for both photometric observations by Huruata et al. (1957) and the spectroscopic one by Struve (1950). Struve (1950) classified its spectral type as A9n, but Duerbeck & Rucinski (2007) reported that the spectral classification of HDH (Michigan Catalogue of HD Stars) is F3V and agrees with the Tycho-2, $B - V = 0.39$ (Hog et al. 2000). The radial-velocity studies by Duerbeck & Rucinski (2007) suggested that TY Pup is a typical A-subtype contact binary with a mass ratio of $q = 0.25$.

Recently, based on V-band observations obtained by the All Sky Automated Survey (ASAS,

Table 1: Coordinates of TY Pup, the comparison, and the check stars.

Targets	name	α_{2000}	δ_{2000}	$mag(V)$	$B - V$	$J - H$
Binary star	TY Pup	07 ^h 32 ^m 46 ^s .3	-20°47′29″.5	8.62	0.39	0.169
The comparison	HD 60342	07 ^h 33 ^m 10 ^s .2	-20°42′13″.1	8.56	-0.06	-0.067
The check	TYC 5991-1892-1	07 ^h 32 ^m 37 ^s .9	-20°45′05″.1	10.21	0.35	0.188

Pojmanski 1997, 2002), the physical parameters of TY Pup were determined by Deb & Singh (2011). Variations in light curves were found, but did not show O’Connell effect (O’Connell 1951). For the orbital period study, times of minimum light of TY Pup were collected and investigated by several authors (e.g. Gu et al. (1993); Berdnikov & Turner (1995)), they gave a linear ephemeris with no changes in the orbital period. However, Qian (2001) found that the period was increasing continuously at a rate of $dP/dt = 1.66 \times 10^{-7} \text{ d yr}^{-1}$. In this paper, we present new CCD observations and their photometric solutions. Then the changes in the orbital period are investigated based on all available eclipse times which shows a combination of a cyclic variation and a continuously increasing period. We detect that TY Pup is a low-mass-ratio and deep contact binary with an additional companion and it may be a progenitor candidate of luminous red novae.

2. New CCD photometric Observations

The first set of light curves of TY Pup in $BV(RI)_C$ bands were carried out for several nights from January to February 2015 with the back illuminated Apogee F42 2048×2048 CCD attached to the 0.6 m Cassegrain reflecting telescope of PROMPT-8¹ robotic telescope. The telescope is located at the Cerro Tololo Inter-American Observatory (CTIO) in Chile. The web-based SKYNET client allowed us to request and retrieve image remotely via the internet. SKYNET system also provided nightly calibration images, including bias, dark, and flat-field images (Layden et al. 2010). All CCD reductions and aperture photometry measurements were done with standard procedure packages of IRAF².

The coordinates of the comparison and check stars are listed in Table 1. The corresponding light curves are displayed in Fig. 1 where the magnitude differences between the comparison star and the check star are shown in the figure. The second set of light curve were obtained from March to April 2017 and plotted in Fig. 2. To obtain more times of light minimum, TY Pup was also monitored by using the 60 cm and 1.0-m telescopes of Yunnan Observatories (YNOs) in February 2015 and January 2018, respectively. These telescopes were equipped with a Cassegrain-focus multicolor CCD photometer where an Andor DW436 2K CCD camera. Standard Johnson-Cousin-Bessel $BV(RI)_C$ filters were used. The eclipse profiles obtained from Yunnan Observatories are shown in Fig. 3. The two sets of photometric data for TY Pup in magnitude differences between the variable star and the comparison star with heliocentric Julian dates are listed in the online Table 2 and 3 for 2015 and 2017, respectively.

¹PROMPT-8 is the Thai Southern Hemisphere Telescope (TST), operated in collaboration between National Astronomical Research Institute of Thailand (NARIT) and the University of North Carolina (UNC) at Chapel Hill in a part of the UNC-led PROMPT project, <http://skynet.unc.edu>.

²The Image Reduction and Analysis Facility (IRAF), <http://iraf.noao.edu>.

Table 2: CCD observations in BVRI bands for TY Pup observed in 2015

HJD -2457000	ΔB mag	HJD	ΔV	HJD	ΔR	HJD	ΔI	HJD	ΔB	HJD	ΔV	HJD	ΔR
39.6317	0.583	39.6321	0.128	39.6325	-0.139	39.6329	-0.386	39.7541	0.220	39.7545	-0.206	39.7549	-0.482
39.6333	0.577	39.6337	0.104	39.6341	-0.152	39.6345	-0.406	39.7558	0.215	39.7562	-0.204	39.7566	-0.477
39.6349	0.571	39.6353	0.107	39.6358	-0.157	39.6362	-0.416	39.7574	0.224	39.7578	-0.208	39.7582	-0.465
39.6367	0.553	39.6371	0.103	39.6375	-0.165	39.6379	-0.427	39.7591	0.206	39.7595	-0.213	39.7599	-0.480
39.6384	0.548	39.6388	0.074	39.6392	-0.176	39.6396	-0.434	39.7608	0.207	39.7612	-0.213	39.7616	-0.494
39.6401	0.551	39.6405	0.078	39.6408	-0.189	39.6413	-0.438	39.7624	0.228	39.7627	-0.221	39.7632	-0.483
39.6417	0.536	39.6422	0.074	39.6426	-0.196	39.6430	-0.423	39.7641	0.211	39.7645	-0.222	39.7649	-0.497
39.6434	0.520	39.6439	0.062	39.6443	-0.200	39.6447	-0.443	39.7658	0.210	39.7662	-0.198	39.7666	-0.492
39.6452	0.516	39.6456	0.050	39.6459	-0.203	39.6463	-0.449	39.7716	0.189	39.7720	-0.232	39.7724	-0.500
39.6468	0.505	39.6472	0.062	39.6476	-0.225	39.6481	-0.452	39.7733	0.200	39.7737	-0.207	39.7741	-0.482
39.6485	0.505	39.6489	0.047	39.6494	-0.214	39.6498	-0.485	39.7750	0.192	39.7754	-0.210	39.7758	-0.488
39.6502	0.486	39.6506	0.041	39.6509	-0.217	39.6514	-0.479	39.7767	0.193	39.7771	-0.209	39.7775	-0.494
39.6518	0.491	39.6522	0.036	39.6527	-0.243	39.6531	-0.486	39.7784	0.191	39.7788	-0.205	39.7792	-0.502
39.6535	0.478	39.6540	0.030	39.6544	-0.219	39.6548	-0.478	39.7801	0.192	39.7805	-0.220	39.7809	-0.507
39.6553	0.472	39.6557	-0.001	39.6561	-0.242	39.6565	-0.484	39.7818	0.195	39.7822	-0.218	39.7826	-0.498
39.6569	0.469	39.6573	0.008	39.6577	-0.238	39.6581	-0.493	39.7835	0.200	39.7839	-0.232	39.7843	-0.493
39.6586	0.459	39.6590	-0.014	39.6594	-0.256	39.6597	-0.515	39.7852	0.172	39.7855	-0.248	39.7860	-0.502
39.6602	0.462	39.6606	-0.010	39.6610	-0.271	39.6614	-0.509	39.7868	0.187	39.7873	-0.209	39.7877	-0.492
39.6619	0.448	39.6623	-0.013	39.6627	-0.269	39.6630	-0.524	39.7885	0.158	39.7889	-0.210	39.7893	-0.474
39.6635	0.445	39.6639	-0.021	39.6643	-0.287	39.6647	-0.534	39.7902	0.190	39.7907	-0.218	39.7912	-0.491
39.6651	0.423	39.6655	-0.031	39.6659	-0.283	39.6665	-0.509	39.7922	0.181	39.7926	-0.222	39.7930	-0.505
39.6683	0.417	39.6692	-0.036	39.6722	-0.307	39.6727	-0.552	39.7939	0.182	39.7944	-0.208	39.7948	-0.479
39.6731	0.418	39.6735	-0.064	39.6739	-0.320	39.6744	-0.558	39.7957	0.166	39.7961	-0.240	39.7965	-0.499
39.6749	0.400	39.6753	-0.070	39.6758	-0.330	39.6762	-0.555	39.7975	0.166	39.7978	-0.221	39.7983	-0.490
39.6767	0.384	39.6771	-0.054	39.6775	-0.311	39.6779	-0.588	39.7992	0.212	39.7996	-0.218	39.8001	-0.478
39.6784	0.391	39.6789	-0.068	39.6792	-0.319	39.6797	-0.558	39.8010	0.204	39.8014	-0.198	39.8019	-0.516
39.6801	0.377	39.6806	-0.074	39.6809	-0.335	39.6813	-0.574	39.8028	0.209	39.8033	-0.224	39.8037	-0.500
39.6818	0.374	39.6822	-0.083	39.6827	-0.339	39.6831	-0.579	39.8227	0.245	39.8232	-0.188	39.8236	-0.468
39.6836	0.365	39.6911	-0.111	39.6972	-0.383	39.6977	-0.626	39.8245	0.238	39.8250	-0.192	39.8253	-0.452
39.6982	0.320	39.6986	-0.119	39.6990	-0.383	39.6995	-0.634	39.8262	0.243	39.8267	-0.169	39.8270	-0.455
39.6999	0.301	39.7004	-0.113	39.7010	-0.383	39.7013	-0.623	39.8279	0.248	39.8283	-0.184	39.8287	-0.478
39.7019	0.303	39.7024	-0.120	39.7028	-0.394	39.7032	-0.640	39.8296	0.230	39.8300	-0.152	39.8305	-0.466
39.7037	0.292	39.7042	-0.119	39.7046	-0.395	39.7050	-0.643	39.8314	0.260	39.8318	-0.189	39.8322	-0.484
39.7055	0.296	39.7060	-0.122	39.7065	-0.406	39.7069	-0.655	39.8331	0.233	39.8335	-0.174	39.8339	-0.451
39.7074	0.293	39.7078	-0.136	39.7082	-0.396	39.7087	-0.648	39.8349	0.250	39.8353	-0.152	39.8357	-0.461
39.7092	0.287	39.7096	-0.130	39.7100	-0.408	39.7104	-0.630	39.8366	0.243	39.8370	-0.181	39.8375	-0.445
39.7110	0.278	39.7115	-0.136	39.7120	-0.412	39.7124	-0.657	39.8384	0.269	39.8388	-0.191	39.8391	-0.455
39.7129	0.286	39.7133	-0.137	39.7137	-0.417	39.7141	-0.646	39.8400	0.254	39.8404	-0.153	39.8408	-0.443
39.7146	0.279	39.7150	-0.149	39.7153	-0.424	39.7157	-0.665	39.8417	0.276	39.8421	-0.178	39.8426	-0.456
39.7163	0.271	39.7167	-0.145	39.7172	-0.419	39.7176	-0.665	39.8434	0.258	39.8438	-0.164	39.8443	-0.450
39.7180	0.263	39.7184	-0.142	39.7188	-0.438	39.7192	-0.663	39.8452	0.281	39.8457	-0.166	39.8461	-0.430
39.7197	0.254	39.7202	-0.167	39.7205	-0.448	39.7210	-0.656	39.8470	0.306	39.8474	-0.154	39.8480	-0.440
39.7215	0.256	39.7220	-0.172	39.7226	-0.425	39.7233	-0.686	39.8489	0.274	39.8493	-0.145	39.8497	-0.399
39.7241	0.250	39.7247	-0.189	39.7251	-0.444	39.7255	-0.681	39.8506	0.294	39.8511	-0.126	39.8516	-0.393
39.7260	0.256	39.7264	-0.167	39.7269	-0.455	39.7274	-0.676	39.8525	0.305	39.8529	-0.114	39.8534	-0.435
39.7279	0.254	39.7284	-0.181	39.7289	-0.439	39.7293	-0.698	39.8544	0.307	39.8548	-0.118	40.7574	-0.179
39.7298	0.236	39.7302	-0.173	39.7308	-0.452	39.7312	-0.705	40.7582	0.542	40.7587	0.101	40.7590	-0.167
39.7318	0.243	39.7322	-0.167	39.7326	-0.445	39.7331	-0.695	40.7599	0.561	40.7603	0.108	40.7607	-0.178
39.7336	0.241	39.7343	-0.194	39.7348	-0.461	39.7352	-0.687	40.7615	0.573	40.7619	0.128	40.7623	-0.130
39.7356	0.242	39.7361	-0.189	39.7364	-0.464	39.7368	-0.698	40.7632	0.575	40.7636	0.129	40.7640	-0.141
39.7373	0.235	39.7377	-0.189	39.7381	-0.444	39.7385	-0.687	40.7649	0.586	40.7653	0.133	40.7656	-0.132
39.7390	0.226	39.7394	-0.190	39.7398	-0.452	39.7402	-0.686	40.7665	0.587	40.7669	0.126	40.7674	-0.140
39.7407	0.228	39.7411	-0.197	39.7415	-0.453	39.7419	-0.709	40.7683	0.587	40.7687	0.130	40.7690	-0.108
39.7423	0.235	39.7427	-0.186	39.7431	-0.474	39.7436	-0.706	40.7699	0.599	40.7703	0.148	40.7707	-0.120
39.7440	0.229	39.7443	-0.189	39.7447	-0.471	39.7451	-0.692	40.7716	0.591	40.7720	0.129	40.7724	-0.111
39.7456	0.231	39.7460	-0.209	39.7464	-0.474	39.7468	-0.703	40.7733	0.603	40.7737	0.154	40.7740	-0.129
39.7472	0.225	39.7476	-0.202	39.7480	-0.481	39.7484	-0.688	40.7749	0.601	40.7753	0.154	40.7757	-0.102
39.7489	0.212	39.7493	-0.205	39.7497	-0.477	39.7501	-0.717	40.7766	0.603	40.7770	0.153	40.7774	-0.108
39.7505	0.224	39.7509	-0.204	39.7513	-0.467	39.7517	-0.721	40.7783	0.611	40.7787	0.150	40.7791	-0.103
39.7522	0.215	39.7526	-0.197	39.7530	-0.474	39.7535	-0.699	40.7800	0.618	40.7804	0.168	40.7808	-0.116

Table 3: CCD observations in BVRI bands for TY Pup observed in 2017

HJD -2457800	ΔB mag	HJD	ΔV	HJD	ΔR	HJD	ΔI	HJD	ΔB	HJD	ΔV	HJD	ΔR
33.6422	0.203	33.6425	-0.238	33.6427	-0.506	33.6430	-0.715	35.5474	0.466	35.5527	-0.009	35.5530	-0.276
33.6439	0.219	33.6441	-0.249	33.6444	-0.502	33.6448	-0.710	35.5489	0.481	35.5542	-0.014	35.5545	-0.275
33.6512	0.210	33.6515	-0.256	33.6517	-0.464	33.6520	-0.720	35.5525	0.453	35.5557	-0.069	35.5560	-0.301
33.6530	0.221	33.6532	-0.222	33.6552	-0.488	33.6537	-0.697	35.5539	0.441	35.5571	-0.052	35.5574	-0.299
33.6546	0.224	33.6549	-0.230	33.6571	-0.478	33.6555	-0.721	35.5553	0.432	35.5589	-0.029	35.5592	-0.304
33.6565	0.203	33.6569	-0.235	33.6588	-0.463	33.6574	-0.722	35.5568	0.441	35.5604	-0.056	35.5607	-0.292
33.6584	0.229	33.6586	-0.229	33.6618	-0.491	33.6591	-0.691	35.5586	0.436	35.5622	-0.020	35.5625	-0.304
33.6611	0.232	33.6614	-0.214	33.6638	-0.471	33.6621	-0.692	35.5600	0.412	35.5636	-0.068	35.5639	-0.284
33.6631	0.241	33.6634	-0.240	33.6670	-0.460	33.6641	-0.697	35.5618	0.418	35.5650	-0.069	35.5653	-0.317
33.6664	0.233	33.6667	-0.222	33.6688	-0.464	33.6673	-0.701	35.5632	0.414	35.5664	-0.068	35.5666	-0.328
33.6683	0.237	33.6686	-0.240	33.6707	-0.473	33.6691	-0.716	35.5646	0.419	35.5679	-0.075	35.5682	-0.323
33.6703	0.245	33.6705	-0.197	33.6960	-0.439	33.6710	-0.694	35.5661	0.402	35.5697	-0.075	35.5700	-0.333
33.6954	0.290	33.6957	-0.180	33.6978	-0.398	33.6962	-0.653	35.5675	0.405	35.5781	-0.087	35.5785	-0.359
33.6972	0.295	33.6976	-0.176	33.6997	-0.384	33.6980	-0.670	35.5693	0.404	35.5797	-0.098	35.5800	-0.359
33.6990	0.293	33.6994	-0.167	34.5324	-0.390	33.6999	-0.652	35.5729	0.383	35.5815	-0.088	35.5818	-0.336
33.7009	0.285	33.7011	-0.125	34.5338	-0.374	34.5326	-0.625	35.5794	0.374	35.5829	-0.108	35.5831	-0.369
34.5331	0.317	34.5334	-0.127	34.5352	-0.384	34.5340	-0.612	35.5811	0.367	35.5842	-0.105	35.5846	-0.381
34.5345	0.313	34.5349	-0.118	34.5367	-0.399	34.5356	-0.619	35.5826	0.357	35.5858	-0.128	35.5861	-0.383
34.5360	0.323	34.5363	-0.153	34.5380	-0.377	34.5369	-0.604	35.5840	0.372	35.5872	-0.111	35.5874	-0.372
34.5374	0.327	34.5377	-0.108	34.5394	-0.362	34.5383	-0.592	35.5854	0.347	35.5886	-0.121	35.5890	-0.381
34.5389	0.332	34.5391	-0.108	34.5409	-0.376	34.5398	-0.591	35.5869	0.363	35.5900	-0.131	35.5903	-0.378
34.5403	0.345	34.5405	-0.128	34.5424	-0.353	34.5411	-0.598	35.5883	0.373	35.5935	-0.117	35.5939	-0.396
34.5417	0.338	34.5421	-0.113	34.5436	-0.375	34.5428	-0.602	35.5897	0.353	35.5951	-0.127	35.5954	-0.388
34.5432	0.348	34.5434	-0.107	34.5465	-0.381	34.5440	-0.596	35.5912	0.337	35.5965	-0.123	35.5969	-0.393
34.5459	0.359	34.5462	-0.109	34.5492	-0.359	34.5495	-0.591	35.5947	0.328	35.5980	-0.132	35.5983	-0.406
34.5486	0.354	34.5490	-0.091	34.5540	-0.349	34.5543	-0.569	35.5962	0.326	35.5998	-0.133	35.6001	-0.394
34.5514	0.373	34.5536	-0.092	34.5569	-0.317	34.5572	-0.564	35.5976	0.325	35.6012	-0.150	35.6015	-0.399
34.5562	0.381	34.5566	-0.068	34.5597	-0.309	34.5599	-0.539	35.5994	0.326	35.6026	-0.136	35.6029	-0.415
34.5591	0.388	34.5593	-0.080	34.5623	-0.315	34.5627	-0.546	35.6008	0.316	35.6041	-0.152	35.6043	-0.406
34.5618	0.395	34.5621	-0.042	34.5650	-0.326	34.5653	-0.557	35.6023	0.317	35.6054	-0.160	35.6057	-0.421
34.5645	0.406	34.5648	-0.068	34.5678	-0.309	34.5681	-0.521	35.6037	0.321	35.6069	-0.153	35.6071	-0.423
34.5672	0.414	34.5703	-0.020	34.5707	-0.304	34.5709	-0.523	35.6051	0.330	35.6084	-0.149	35.6087	-0.409
34.5700	0.426	34.5750	-0.033	34.5752	-0.280	34.5755	-0.486	35.6066	0.305	35.6098	-0.156	35.6101	-0.409
34.5727	0.440	34.5791	-0.001	34.5793	-0.260	34.5797	-0.488	35.6080	0.303	35.6116	-0.172	35.6119	-0.418
34.5788	0.442	34.5819	0.035	34.5821	-0.254	34.5823	-0.496	35.6094	0.300	35.6149	-0.169	35.6151	-0.433
34.5815	0.461	34.5916	0.059	34.5918	-0.208	34.5920	-0.465	35.6112	0.292	35.6162	-0.167	35.6166	-0.436
34.5912	0.510	34.6098	0.129	34.6101	-0.125	34.6105	-0.369	35.6127	0.299	35.6180	-0.174	35.6183	-0.443
34.5939	0.520	34.6153	0.150	34.6129	-0.122	34.6131	-0.342	35.6159	0.291	35.6194	-0.181	35.6198	-0.430
34.6123	0.594	34.6200	0.160	34.6174	-0.113	34.6177	-0.352	35.6177	0.282	35.6209	-0.165	35.6212	-0.447
34.6149	0.600	34.6364	0.160	34.6202	-0.108	34.6204	-0.333	35.6191	0.279	35.6223	-0.174	35.6227	-0.449
34.6175	0.607	34.6410	0.147	34.6385	-0.095	34.6444	-0.311	35.6205	0.276	35.6241	-0.183	35.6243	-0.452
34.6361	0.610	34.6437	0.132	34.6413	-0.109	34.6470	-0.328	35.6220	0.272	35.6256	-0.206	35.6259	-0.444
34.6406	0.615	34.6465	0.165	34.6441	-0.125	34.6514	-0.324	35.6238	0.265	35.6273	-0.201	35.6277	-0.448
34.6434	0.608	34.6508	0.158	34.6468	-0.095	34.6541	-0.323	35.6252	0.274	35.6288	-0.196	35.6291	-0.462
34.6462	0.607	34.6536	0.171	34.6510	-0.093	35.5322	-0.406	35.6270	0.272	35.6302	-0.183	35.6305	-0.446
34.6505	0.612	34.6563	0.155	34.6538	-0.087	35.5335	-0.420	35.6284	0.263	35.6316	-0.202	35.6320	-0.463
34.6532	0.608	35.5301	0.076	35.5303	-0.183	35.5365	-0.454	35.6299	0.264	35.6330	-0.210	35.6333	-0.460
34.6560	0.623	35.5316	0.087	35.5319	-0.168	35.5380	-0.443	35.6313	0.256	35.6364	-0.195	35.6367	-0.470
35.5298	0.536	35.5330	0.075	35.5333	-0.198	35.5393	-0.460	35.6327	0.266	35.6381	-0.216	35.6384	-0.483
35.5313	0.539	35.5345	0.073	35.5349	-0.212	35.5409	-0.440	35.6360	0.251	35.6399	-0.215	35.6402	-0.485
35.5327	0.535	35.5358	0.060	35.5362	-0.221	35.5422	-0.454	35.6378	0.251	35.6423	-0.198	35.6426	-0.453
35.5342	0.524	35.5374	0.034	35.5377	-0.204	35.5437	-0.472	35.6396	0.240	35.6445	-0.234	35.6449	-0.461
35.5356	0.526	35.5387	0.023	35.5391	-0.208	35.5450	-0.472	35.6419	0.249	35.6460	-0.229	35.6462	-0.476
35.5371	0.504	35.5403	0.030	35.5406	-0.223	35.5467	-0.476	35.6443	0.231	35.6476	-0.226	35.6479	-0.483
35.5385	0.502	35.5417	0.035	35.5419	-0.217	35.5484	-0.494	35.6456	0.229	35.6494	-0.236	35.6498	-0.474
35.5399	0.510	35.5430	0.028	35.5434	-0.240	35.5518	-0.475	35.6474	0.233	35.6513	-0.224	35.6516	-0.499
35.5414	0.486	35.5446	0.018	35.5448	-0.235	35.5534	-0.489	35.6491	0.219	35.6531	-0.225	35.6535	-0.475
35.5428	0.487	35.5460	0.040	35.5464	-0.244	35.5548	-0.508	35.6509	0.225	35.6550	-0.218	35.6553	-0.473
35.5442	0.488	35.5478	0.017	35.5481	-0.246	35.5563	-0.500	35.6528	0.230	35.6567	-0.252	35.6571	-0.506
35.5457	0.455	35.5511	-0.001	35.5514	-0.277	35.5578	-0.522	35.6546	0.223	35.6585	-0.227	35.6588	-0.497

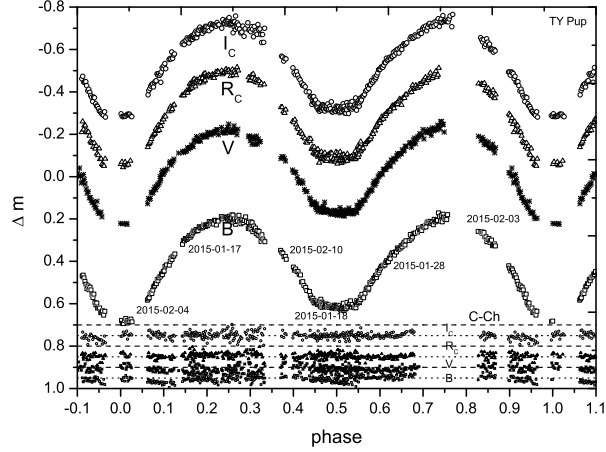


Fig. 1.— Multi-color CCD light curves in B , V , $(RI)_c$ bands obtained with the 0.6-m telescope at CTIO in January and February 2015. The differential magnitudes between the comparison and the check stars are also presented.

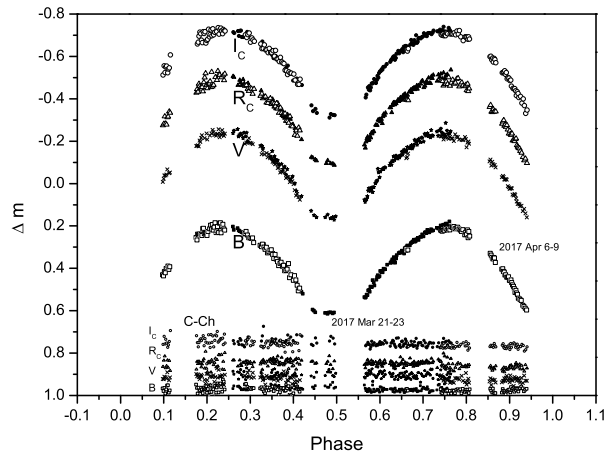


Fig. 2.— CCD photometric observations in B , V , $(RI)_c$ bands were obtained with the 0.6-m telescope at CTIO in March and April 2017. As those shown in Fig. 1, the magnitude differences between the comparison and the check stars are shown.

3. Variations in the orbital period

Earlier epochs and $O - C$ analyses of TY Pup were published by several investigators (e.g. Gu et al. 1993 and Berdnikov & Turner 1995). The authors derived a linear ephemeris for the binary. Later, Qian (2001a) obtained a quadratic ephemeris and pointed out that the period of TY Pup was secular increasing with rate of $dP/dt = 1.66 \times 10^{-7} \text{ d yr}^{-1}$ and $\dot{P}/P = 2.03 \times 10^{-7} \text{ yr}^{-1}$.

Based on our photometric observations, four times of light minimum were determined. All times of minimum light are listed in Table 4. The variations of the orbital period were analysed by using $O - C$ (observed minus calculated) method. In order to investigate the orbital period change of TY Pup, the $(O - C)_1$ values of all available times of light minimum were computed with the linear ephemeris given by Kreiner (2004):

$$\text{Min.}I(HJD) = 2434412.106 + 0^d.8192423 \times E. \quad (1)$$

The corresponding O-C diagram is shown in the upper panel of Fig. 4. As shown in the panel, the changes in the orbital period of TY Pup are complex due to a small-amplitude cyclic variation and an upward parabolic variation cannot fit the $(O - C)_1$ curve very well. To get a better fit for the trend of $(O - C)_1$ curve, we have to combine a new quadratic ephemeris with an additional sinusoidal term. By using a least-squares method, the new ephemeris was determined:

$$\begin{aligned} \text{Min.}I(HJD) &= 2434412.1128(\pm 0.0002) + 0.8192406(\pm 0.0000003)E \\ &+ [62.5(\pm 0.9) \times 10^{-12}]E^2 \\ &+ 0.0072(\pm 0.0001) \times \sin[0.^{\circ}2229E + 60.^{\circ}0(\pm 0.^{\circ}9)]. \end{aligned} \quad (2)$$

According to Eq. (2), the semi-amplitude of cyclic oscillation is 0.0072 days and the sinusoidal term suggests an oscillation period of 3.62 years. The quadratic term in Eq. (2) also reveals a continuous period increase at a rate of $dP/dt = 5.57(\pm 0.08) \times 10^{-8} \text{ d yr}^{-1}$. This kind of period variation is usually encountered for W UMa-type binary stars. Some other examples are AB And and TY UMa (e.g., Li et al. 2014, 2015). After the long-term period change is subtracted from the O-C diagram, the cyclic oscillation is shown in the middle panel of Fig. 4. The residuals of Eq. (2) are plotted in the lowest panel. However, there are no times of light minimum recorded between $E=0$ and $E=14250$, thus new eclipse times are required in the future to confirm the variations presented here.

4. Photometric solutions with W-D method

The light curve of W UMa-type binary stars are usually varying with time. Some examples with variable light curves are FG Hya (Qian & Yang 2005), AD Cnc (Qian et al. 2007), BX Peg (Lee et al. 2004), CU Tau (Qian et al. 2005), CE Leo (Kang et al. 2004), EQ Tau (Yuan & Qian, 2007), and QX And (Qian et al. 2007). To check whether the light curve of TY Pup is variable or not, we compare our light curves obtained in 2015 and 2017 as shown in Fig. 5, the light curves

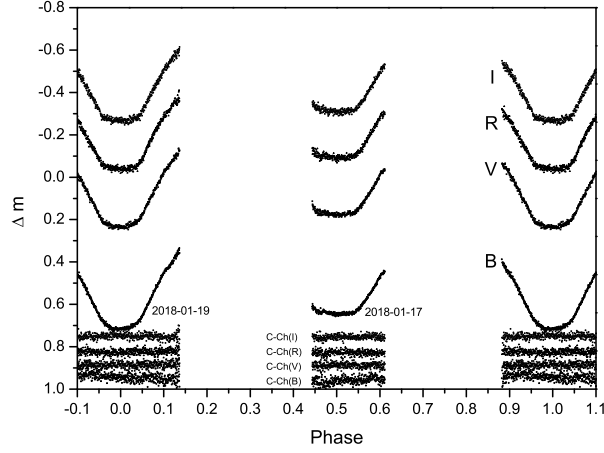


Fig. 3.— Eclipse profiles in B , V , R and I bands were obtained with the 1.0-m telescope at YNOs in January 2018.

Table 4: Times of minimum light for TY Pup.

HJD(2400000+)	Error(days)	E	$(O - C)_1$	Method	Min	Ref.
34092.6040	0.0009	-390.0	0.0025	pe	I	(1)
34412.1060		0.0	0.0000	pe	I	(4)
34416.2056	0.0008	5.0	0.0034	pe	I	(1)
46086.2934		14250.0	-0.0154	pe	I	(2)
46087.1161		14251.0	-0.0119	pe	I	(2)
46100.2230	0.0002	14267.0	-0.0129	pe	I	(2)
46107.1867		14275.5	-0.0128	pe	II	(2)
48500.6190		17197.0	0.0032	ccd	I	(5)
49817.1362	0.0013	18804.0	-0.0020	pe	I	(3)
51508.0490		20868.0	-0.0053	ccd	I	(5)
51868.9321	0.0013	21308.5	0.0016	ccd	II	(6)
51869.3383	0.0013	21309.0	-0.0018	ccd	I	(6)
53714.2755		23561.0	0.0017	ccd	I	(5)
53778.9938		23640.0	-0.0002	ccd	I	(5)
54120.6157		24057.0	-0.0023	ccd	I	(5)
56323.9812		26746.5	0.0110	ccd	II	(5)
56714.3402	0.0003	27223.0	0.0011	ccd	I	(7)
56730.3147	0.0005	27242.5	0.0003	ccd	II	(7)
56737.2797	0.0003	27251.0	0.0018	ccd	I	(7)
57028.5180		27606.5	-0.0006	ccd	II	(5)
57033.0229		27612.0	-0.0015	ccd	I	(5)
57040.8097	0.0013	27621.5	0.0025	ccd	II	PROMPT-8
57080.1451	0.0004	27669.5	0.0143	ccd	II	YNOs 60-cm
58136.1354	0.0006	28958.5	0.0013	ccd	II	YNOs 1.0-m
58138.1842	0.0002	28961.0	0.0020	ccd	I	YNOs 1.0-m

References. (1) Huruhata et al. 1957; (2) Gu et al. 1993; (3) Berdnikov & Turner 1995; (4) Van Houten 1971; (5) <http://var.astro.cz/ocgate>; (6) Pojmanski 1997 & 2002; (7) Karampotsiou et al. 2016.

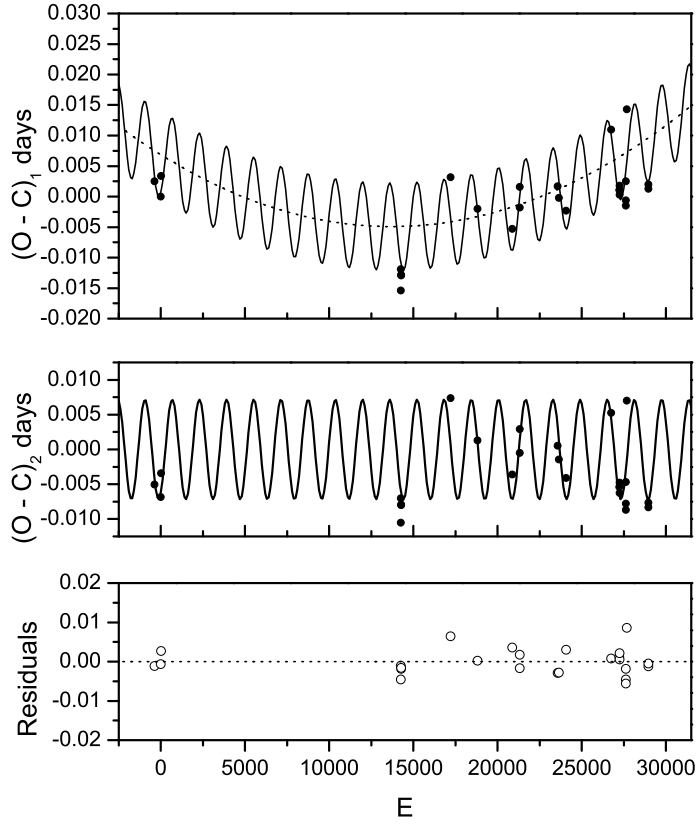


Fig. 4.— The $(O - C)_1$ diagram was constructed by using the linear ephemeris in Eq. (1). The solid line in the upper panel refers to a combination of a long-term period increase and a semi-amplitude cyclic oscillation, while the dashed line refers to the long-term increase.

generally overlap within the error and all of them are clearly symmetric indicating that the light curve may not be variable.

For the photometric solution, we use the spectral type of F3V determined by Duerbeck & Rucinski (2007). Our photometric data in four-color $BV(RI)_C$ light curves observed in 2015 are analysed by using the Wilson & Devinney (W-D) code (Wilson & Devinney 1971; Wilson 1990, 1994, 2012; van Hamme & Wilson 2007) to determine their photometric elements. The color index $B - V = 0.40$ given by Morton & Adams (1968) corresponds to $T_{eff} = 7000$ K, while the value $B - V = 0.39$ where $T_{eff} = 6900$ K (Flower 1996). During the solutions, the effective temperature of the primary star (T_1) was fixed as 6900 K corresponding to its spectral type (Cox 2000). We assume that the convective envelope is already developed for both components. Therefore, the bolometric albedos for star 1 and 2 were taken as $A_1 = A_2 = 0.5$ (Rucinski 1969) and the values of the gravity-darkening coefficients $g_1 = g_2 = 0.32$ (Lucy 1967) were used. The monochromatic and bolometric limb-darkening coefficients were logarithmically interpolated from van Hamme’s table (van Hamme 1993).

Ideally, for reliable masses the mass ratio should be obtained from precise spectroscopic radial velocity measurements (Deb & Singh 2011). But for our photometric data, we found that the synthetic light curves could not fit well when we used the spectroscopic mass ratio q_{sp} of 0.25 ± 0.03 from Duerbeck & Rucinski (2007). Therefore, We used a q -search method to determine its photometric mass ratio q_{ph} and then set the mass ratio as an adjustable parameter to get a better fit. The q -search result suggests that the range of mass ratio is between 0.18 to 0.22 as displayed in Fig. 7. At the end of modeling process, we obtained the photometric mass ratio of $0.1839 (\pm 0.0016)$ at the lowest sum of the weighted square deviations $\Sigma(\omega(O - C))^2$ or hereafter Σ .

The adjustable parameters are the inclination (i), the mass ratio (q), the temperature of Star 2 (T_2), the monochromatic luminosity of Star 1 (L_{1B} , L_{1V} , L_{1R} and L_{1I}), the dimensionless potential of stars 1 ($\Omega_1 = \Omega_2$) in mode 3 (Leung & Willson 1977) for contact configuration, respectively. As shown in Fig. 5, the light curves in $BV(RI)_C$ bands seem to be symmetric, so no spot model was considered. In addition, the $(O - C)$ diagram shows a cyclic variation that may be caused by light-travel time effect via the presence of a third companion. Thus, we added the third light (l_3) as an adjustable parameter in the modeling process to get a better fit. As the result, the third light could not be detected during the process. It seems to be very small contribution when compared to the total light from the system. The solutions are listed in Table 5 and theoretical light curves (solid lines) are plotted in Fig. 8, compared to the normal points from photometric observations.

5. Discussions and conclusions

Although TY Pup was discovered in 1928 as a variable star, it was neglected for photometric study and orbital period investigation. Our photometric solutions indicate that TY Pup is an A-subtype deep-contact binary with a high fill-out factor ($f = 84.3\%$) and a low mass ratio ($q =$

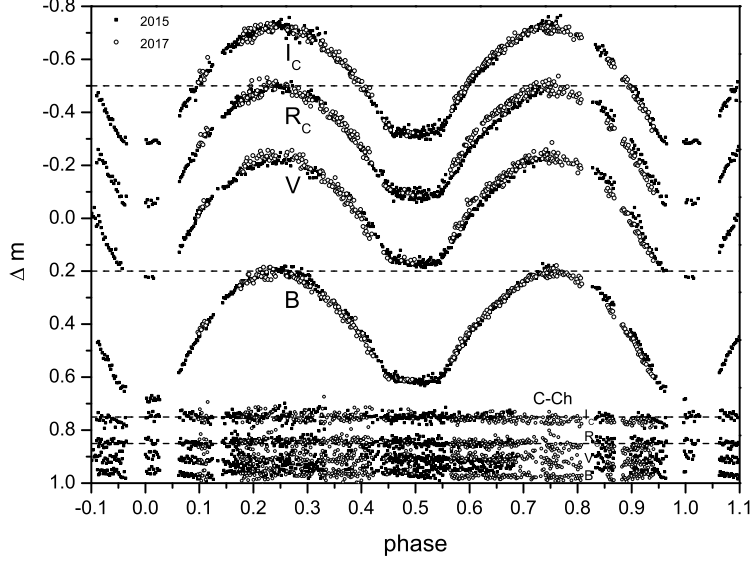


Fig. 5.— The comparison between our light curves obtained during 2015 and 2017 in B , V , R_C and I_C bands.

Table 5: Photometric solutions with formal errors.

Parameters	Data (2015)
$T_1(K)$	6900 (fixed)
$g_1 = g_2$	0.32 (fixed)
$A_1 = A_2$	0.50 (fixed)
q	0.1839(± 0.0016)
$T_2(K)$	6915(± 10)
$i(^{\circ})$	83.638(± 0.189)
Ω_{in}	2.1923
Ω_{out}	2.0745
$\Omega_1 = \Omega_2$	2.0930(± 0.0049)
$L_1/(L_1 + L_2)(B)$	0.7982(± 0.0015)
$L_1/(L_1 + L_2)(V)$	0.7996(± 0.0011)
$L_1/(L_1 + L_2)(R)$	0.8004(± 0.0009)
$L_1/(L_1 + L_2)(I)$	0.8010(± 0.0009)
$r_1(pole)$	0.5181(± 0.0009)
$r_1(side)$	0.5753(± 0.0014)
$r_1(back)$	0.6060(± 0.0014)
$r_2(pole)$	0.2568(± 0.0044)
$r_2(side)$	0.2720(± 0.0056)
$r_2(back)$	0.3564(± 0.0260)
f	84.3%($\pm 4.1\%$)
$\Sigma W(O - C)^2$	0.0059

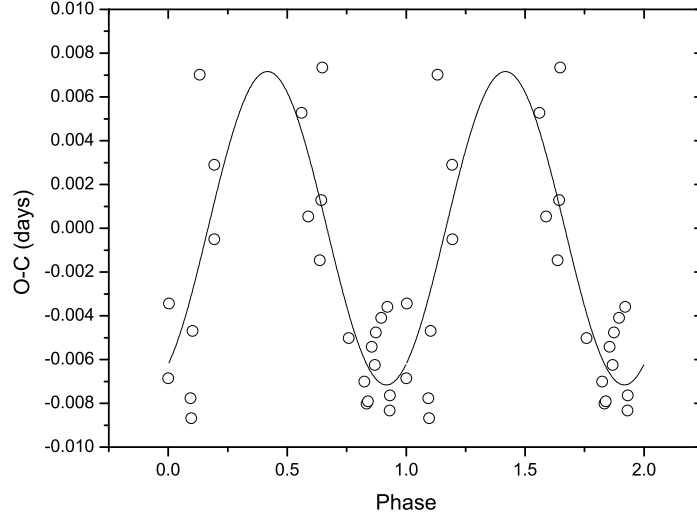


Fig. 6.— The variation in orbital period from middle panel of Fig. 4 as phase scale. The computed curve almost covers to all $O - C$ data, the maxima and the minima are quite constrained to the curve, indicating that the period change is reliable.

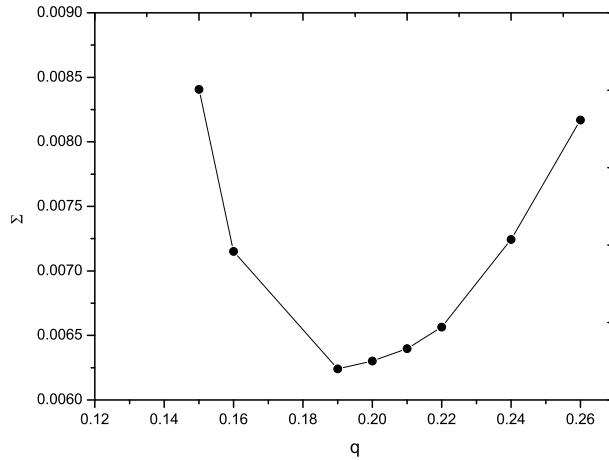


Fig. 7.— Relation between the mass ratio q and the sum of weighted square deviations (Σ). The graph indicates that the optimal mass ratio q is in the range between 0.18 and 0.22.

0.184). These parameters are close to those derived by Gu et al. (1993) and Deb & Singh (2011), while the photometric mass ratio differs from the spectroscopic one $q = 0.25$ given by Duerbeck & Rucinski (2007). This may be caused by the fact that the radial-velocity curves of TY Pup given by them were constructed by only a few observations. As we can see in Fig. 4 in the paper of Duerbeck & Rucinski, the spectroscopic mass ratio mainly depended on one data point. The temperature difference of the two components is very small ($\Delta T=15$ K) with $T_2/T_1 = 1.0022$, this suggests that the system is in thermal contact. In addition, the orbital inclination is about 83.6 deg, this indicates that it is a total eclipsing binary and physical parameters we obtained are reliable. The geometrical structure of TY Pup is plotted in Fig 9. Based on spectroscopic elements determined by Duerbeck & Rucinski (2007), the absolute parameters of TY Pup are estimated as: $M_1 = 1.650M_\odot$, $M_2 = 0.303M_\odot$, $a = 4.653R_\odot$, $R_1 = 2.636R_\odot$, $R_2 = 1.373R_\odot$, $L_1 = 14.112L_\odot$ and $L_2 = 3.862L_\odot$.

The upward parabolic variation in the O-C diagram reveals that the period of TY Pup is increasing continuously at a rate of $dP/dt = 5.57(\pm 0.08) \times 10^{-8}$ days/year. The period increase can be explained by the mass transfer from the secondary component to the primary one. When material is exchanged between the stars in the system, the center of mass of the system will be shifted and consequently the orbital period of the system will change. If the long-term period increase is due to conservative mass transfer from the less massive component to the more massive one, the mass transfer rate can be determined with the following equation (Tout & Hall 1991),

$$\frac{\dot{P}}{P} = 3 \frac{\dot{M}_2}{M_2} \left(1 - \frac{M_2}{M_1}\right). \quad (3)$$

The result is $dM_2/dt = 8.41 \times 10^{-9} M_\odot \text{yr}^{-1}$. The timescale of mass transfer can be estimated as $M_2/\dot{M}_2 \sim 3.6 \times 10^7 \text{yrs}$ and the time scale of period increase $P/(dP/dt) \sim 1.47 \times 10^7 \text{yrs}$ or $\dot{P}/P \sim 6.8 \times 10^{-8} \text{yr}^{-1}$. If the more massive star (M_1) is gaining mass from the less massive star (M_2), the mass ratio of the contact binary (q) will decrease. The primary will become too massive (Qian 2001b). However, the contact configuration cannot be broken, due to its deep contact configuration

Table 6: Parameters of high fill-out and low mass ratio W UMa binaries.

Star	Spec.	Period (days)	q	f	dP/dt ($\times 10^{-8}$ d/y)	Cyclic	l_3	M_1 (M_\odot)	M_2 (M_\odot)	M_3 (M_\odot)	Ref.
II UMa	F5	0.8252	0.172	86.6%	+48.8	no	yes	1.99	0.34	1.34	(1)
V2388 Oph	F3V	0.8023	0.186	65.0%						0.54	(2)
MW Pav	F3V	0.7949	0.222	60.0%	+0.06	no	yes	1.51	0.33		(3)
MQ UMa	F7V	0.4760	0.195	82.0%		yes	yes	1.33	0.28	F5V	(4)
V409 Hya	F2V	0.4723	0.216	60.6%	+54.1	no	no	1.50	0.33		(5)
V728 Her	F3	0.4713	0.158	81.0%	+19.2	yes	yes	1.80	0.28	0.40	(6)(7)
V776 Cas	F2V	0.4404	0.130	64.6%		yes	yes	1.55	0.20	1.04	(8)
EF Dra	F9V	0.4240	0.160	45.5%		yes	yes	1.81	0.29	0.75	(9)
TY Pup	F3V	0.8192	0.184	84.3%	+5.57	yes	no	1.65	0.30	1.12	this study

Notes. (1) Zhou et al. 2016, (2) Zasche et al. 2014, (3) Alvarez et al. 2015, (4) Zhou et al. 2015, (5) Na et al (2014), (6) Erkan & Ulas 2016, (7) Yu et al 2016, (8) Zhou et al. 2016a., (9) Pribulla et al. 2001

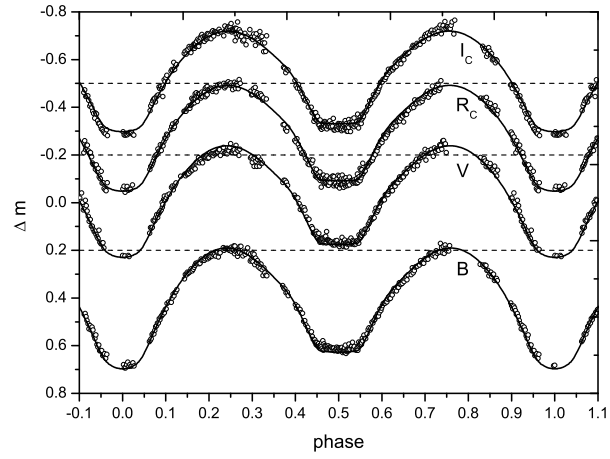


Fig. 8.— Theoretical light curves (solid lines) calculated using the W-D method compare to the normal points of the observed light curves from photometric data in January-February 2015.

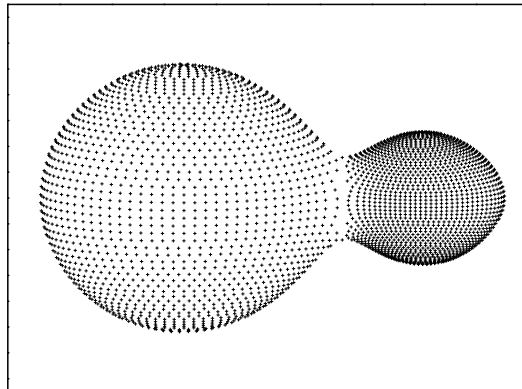


Fig. 9.— Geometrical configuration of TY Pup at phase 0.25

with a high fill-out factor, $f > 50\%$ (He et al. 2012). By using the statistical relation between f and q for low-mass-ratio and deep contact binaries derived by Yang & Qian (2015),

$$f(\%) = 117.6(\pm 7.5) - 527.6(\pm 2.5) \times q + 1164.9(\pm 7.4) \times q^2, \quad (4)$$

a calculation with the mass ratio $q=0.184$ yields the fill-out factor of TY Pup as $f = 59.96\%$. This is smaller than the observed value ($f = 84.3\%$).

The low mass ratio together with the deep contact configuration of TY Pup indicate that it is at the late evolutionary state of contact binaries. According to Hut (1980), when the W UMa system meets a secular tidal instability, i.e., the orbital angular momentum is less than three times of the spin angular momentum ($J_{orb} < 3J_{spin}$), the system will ultimately merge to be a single rapidly rotating star. A computation with the relation between the mass ratio and the angular momentum ratio ($q - J_{spin}/J_{orb}$) given by Yang & Qian (2015),

$$J_{spin}/J_{orb} = 0.5104(\pm 0.0006) - 3.7738(\pm 0.0027) \times q + 8.2817(\pm 0.0081) \times q^2 \quad (5)$$

leads to the angular momentum ratio for TY Pup as 0.096. The decrease of q caused by the mass transfer from the less massive component to the more massive one will cause the system finally meet $J_{spin}/J_{orb} > 1/3$. At that time, the binary will be merging and produce a luminous red nova (e.g., Zhu et al. 2016). Some contact binary systems with observational properties similar to TY Pup are listed in Table 6. All of them are F-type deep contact system with mass ratios lower than 0.25 and fill-out factors larger than 50% (Qian et al. 2005). They may be the progenitor of a single rapid-rotating star and will produce luminous red novae (e.g., Zhu et al. 2016; Sriram et al., 2016, 2017; Liao et al. 2017; Samec et al. 2011, 2018).

The cyclic variation of $O - C$ diagram in Fig 4 can be explained as magnetic activity cycles which normally occur in the late-type stars (e.g. Applegate 1992). However, as discussed by Qian (2001a, 2003), magnetic braking in high fill-out over-contact binaries may be weaker than that in shallow contact binaries. Furthermore, since TY Pup have been found and investigated for decades, no magnetic activity was found from available publications (e.g. Stepien et al. 2001). In addition, it is clear that the variation is periodic, so this variation may be more plausibly interpreted as the light-travel time effect (LTTE) via the presence of a third body. Therefore, we thought that

Table 7: Parameters of a third body

Parameters	Value	Error	Units
A_3	0.0072	0.0001	days
P_3	3.62	0.0000	yrs
$a'_{12} \sin i'$	1.25	0.02	AU
$f(m_3)$	0.148	0.006	M_\odot
e_3	0.0	assumed	-
$M_3 (i' = 90^\circ)$	1.117	0.020	M_\odot
$a_3 (i' = 90^\circ)$	2.178	0.050	AU

the unseen tertiary may be the reason to cause the cyclic oscillation. To derive the parameters of the third component, we assumed that the tertiary’s orbit is circular. The parameters of the third component were determined by using the mass function equation,

$$f(m) = \frac{4\pi^2}{GP_3^2} \times (a'_{12} \sin i')^3 = \frac{(M_3 \sin i')^3}{(M_1 + M_2 + M_3)^2}, \quad (6)$$

where the projected radius of the orbit $a'_{12} \sin i' = A_3 \times c$ (when A_3 is the semi-amplitude of the $O-C$ oscillation, c is the speed of light and i' is the inclination of the orbit of the third component). The corresponding results are shown in Table 7.

The lowest mass of the tertiary $M_3 \sim 1.12 M_\odot$ (at $i' = 90$). It should be very bright and easily detected with either in photometry and spectroscopy as the same V779 Cas (Zhou et al. 2016a). If the tertiary really exists, it may play an important role for the binary formation and evolution by removing angular momentum from the central binary through Kozai oscillation (Kozai 1962) during the early dynamical interaction or late evolution as discussed by Qian et al.(2007, 2013). However, the photometric solution suggests that the contribution of the third light to the total light of the system is very small. Additionally, no third lights were reported from previous photometric investigations (e.g. Gu et al. 1993; Deb & Singh 2011). Moreover, no spectroscopic signal of a third component was detected (e.g. Pribulla & Rucinski 2006; Duerbeck & Rucinski 2007; D’Angelo et al. 2006; Rucinski et al. 2013) or from APOGEE spectra (e.g. El-Badry et al. 2018). Other investigations by Rucinski et al. (2007) and Zakirov (2010) also showed no third body in the binary. It is possible that the third body might be a compact object. The other possibility is that it may be a close binary containing two very faint component stars. More evidence is needed to prove the existence of a third body in the future.

This work is supported by the National Natural Science Foundation of China (No. 11703082). We would like to thank Dr. Wiphu Rujopakarn and NARIT, Thailand for time allocation to use PROMPT-8 for our observations, some observations were obtained by using the 60-cm and 1.0-m telescopes at Yunnan Observatories, China.

REFERENCES

- Alvarez, G. E., Sowell, J. R., Williamon, R. M., Lapasset, E. 2015, *PASP*, 127, 742
- Applegate, J. H. 1992, *A&A*, 385, 621
- Berdnikov, L. N. & Turner, D. G. 1995, *IBVS*, No. 4214
- Campbell, L. 1928 *Harvard Bull.*, No. 858
- Cox, A. N. 2000, *Allen’s astrophysical quantities*, 4th ed. AIP Press(Springer), New York

- D'Angelo, C., van Kerkwijk, M. H. & Rucinski, S. M. 2006, *AJ*, 132, 650
- Deb, S. & Singh, H. P. 2011, *MNRAS*, 412, 1787
- Duerbeck, H. W. & Rucinski, S. M. 2007, *AJ*, 133, 169
- El-Badry, K., Ting, Y.-S., Rix, H.-W., et al. 2018, *MNRAS*, 476, 528
- Erkan, N. & Ulas, B. 2016, *NewA*, 46, 73
- Flower, P. J., 1996, *ApJ*, 469, 355
- Gu, S.-H., Yang, Y., Liu, Q.-Y. and Zhang, Z. 1993, *Ap&SS*, 203, 161
- He, J.-J., Qian, S.-B., Soonthornthum, B. 2012, *ASP Conf. Series*, 451
- Hertzprung, E. 1928, *Bull. Astron. Inst. Netherlands*, 4, 153
- Hog, E., Fabricius, C., Makarov, V. V. et al. 2000, *A&A*, 355, 27
- Huruhata, M., Kitamura, M., Nakamura, T., Tanabe, H. 1957, *Ann. Tokyo Astron. Obs.*, 2nd series, 5, 31
- Hut, P. 1980, *A&A*, 92, 167
- Kandulapati, S., Devarapalli, S. P., Pasagada, V. R. 2015, *MNRAS*, 446, 510
- Karampotsiou, E., Gazeas, K., Petropoulou, M., Tzouganatos, L. 2016, *IBVS*, No. 6158
- Kozai, Y. 1962, *AJ*, 67, 591
- Kreiner, J. M. 2004, *Acta Astron.*, 54, 207
- Layden, A. C. & Broderick, A. J. 2010, *PASP*, 122, 1000
- Leung, K. C., Wilson, R. E. 1977, *ApJ*, 211, 853
- Li, K., Hu, S.-M., Chen, X., Guo, D.-F., 2017, *PASJ*, 69, 79
- Li, K., Hu, S.-M., Guo, D.-F., Jiang, Y.-G. et al. 2015, *AJ*, 149, 120
- Li, K., Hu, S.-M., Jiang, Y.-G., Chen, X., Ren, D.-Y. 2014, *NewA*, 30, 64
- Liao, W.-P., Qian, S.-B., Soonthornthum, B., Sarotsakulchai, T., Zhu, L.-Y., Zhang, J., Irina, Voloshina, 2017, *PASP*, 129, 124204
- Lucy, L. B. 1967, *ZA.*, 65, 89
- Molnar, L. A., Van Noord, D. M., Kinemuchi, K. et al. 2017, *ApJ*, 840, 1

- Morton, D. C. & Adams, T. F. 1968, *ApJ*, 151, 611
- Na, W.-W., Qian, S.-B., Zhang, L., Liao, W.-P., Soonthornthum, B., et al. 2014, *NewA*, 30, 105
- O’Connell, D. J. K., 1951, *Pub. Riverview College Obs.*, 2, 85
- Pojmanski, G. 1997, *Acta Astron.*, 47, 467
- Pojmanski, G. 2002, *Acta Astron.*, 52, 397
- Pribulla, T. & Rucinski, S. M. 2006, *AJ*, 131, 2986
- Pribulla, T., Vanko, M., Chochol, D., Parimucha, S. 2001, *CoSka*, 31, 26
- Qian, S.-B., He, J.-J., Zhang, J., Zhu, L.-Y., Shi, X.-D., Zhao, E.-G., Zhou, X., 2017, *RAA*, 17, 87
- Qian, S.-B., Zhang, J., He, J.-J., Zhu, L.-Y., Zhao, E.-G., Shi, X.-D., Zhou, X., Han, Z.-T., 2018, *ApJS*, 235, 5
- Qian, S.-B., Yang, Y.-G., Soonthornthum, B., Zhu, L.-Y., He, J.-J., Yuan, J.-Z., 2005, *AJ*, 130, 224
- Qian, S.-B. 2001a, *MNRAS*, 328, 635
- Qian, S.-B. 2001b, *MNRAS*, 328, 914
- Qian, S.-B. 2003, *MNRAS*, 342, 1260
- Qian, S.-B. Xiang, F.-Y., Zhu, L.-Y., et al. 2007, *AJ*, 133, 357
- Qian, S.-B. Liu, N.-P. Li, K. et al. 2013, *ApJS*, 209, 13
- Rucinski, S. M. 1969, *Acta Astron.*, 19, 245
- Rucinski, S. M., Pribulla, T. & Budaj, J. 2013, *AJ*, 146, 70
- Rucinski, S. M., Pribulla, T. & van Kerkwijk, M. H. 2007, *AJ*, 134, 2353
- Samec, R., Caton, D., Robb, R., Faulkner, D. R., 2018, *RNAAS*, 2, 13
- Samec, R. G., Labadorf, C. M., Hawkins, N. C., Faulkner, D. R., Van Hamme, W., 2011, *AJ*, 142, 117
- Sriram, K., Malu, S., Choi, C. S., Vivekananda Rao, P., 2016, *AJ*, 151, 69
- Sriram, K.; Malu, S.; Choi, C. S.; Vivekananda Rao, P., 2017, *AJ*, 153, 231
- Stepien, K. 2011, *A&A*, 531, A18
- Stepien, K., Schmitt, J. H. M. M. & Voges, W. 2001, *A&A*, 370, 157

- Struve, O. 1950, ApJ, 112, 184
- Tout, C. A., Hall, D. S., 1991, MNRAS, 253, 9
- Tylenda, R., Hajduk, M., Kaminski, T., et al. 2011, A&A, 528, A114
- Van Hamme, W. 1993, AJ, 106, 2096
- Van Hamme, W. & Wilson, R. E. 2007, ApJ, 661, 1129
- Van Houten, C. J. 1971, A&A, 14, 487
- Wilson, R. E. 1990, ApJ, 356, 613
- Wilson, R. E. 1994, PASP, 106, 921
- Wilson, R. E. 2012, AJ, 144, 73
- Wilson, R. E. & Devinney, E. J. 1971, ApJ, 166, 605
- Yang, Y.-G. & Qian, S.-B. 2015, AJ, 150, 69
- Yu, Y.-X., Xiang, F.-Y. & Hu, K. 2016, PASP, 128, 044202
- Zakirov, M. M. 2010, Kinematics & Physics of Celestial Bodies, 26, 269
- Zasche, P., Uhlar, R. & Svoboda, P. 2014, Acta Astron., 64, 125
- Zhou, X., Qian, S.-B., Liao, W.-P., Zhao, E.-G., Wang, J.-J., Jiang, L.-Q. 2015, AJ, 150, 83
- Zhou, X., Qian, S.-B., Zhang, J., Jiang, L.-Q., Zhang, B., Kreiner, J. 2016a, ApJ, 817, 133
- Zhou, X., Qian, S.-B., Zhang, J., Zhang, B., Kreiner, J. 2016b, AJ, 151, 67
- Zhu, L.-Y., Zhao, E.-G., Zhou, X., 2016, RAA, 16, 68